EUROFUSION WPPMI-CP(16) 14994

MR Gilbert et al.

Activation, decay heat, and waste classification studies of the European DEMO concepts

Preprint of Paper to be submitted for publication in
Proceedings of 26th IAEA Fusion Energy Conference

This work has been carried out within the framework of the EUROfusion Consortium and has received funding from the Euratom research and training programme 2014-2018 under grant agreement No 633053. The views and opinions expressed herein do not necessarily reflect those of the European Commission.

Activation, Decay Heat, and Waste Classification Studies of the European DEMO Concept

M.R. Gilbert[1], T. Eade[1], C. Bachmann[2], U. Fischer[3] and N.P. Taylor[1]

[1]CCFE, Culham Science Centre, Abingdon, Oxfordshire, OX14 3DB, UK
[2]Eurofusion PMU, Boltzmannstr.2, Garching 85748, Germany
[3]Association KIT-Euratom, Karlsruhe Institute of Technology (KIT), Karlsruhe, Germany

Corresponding Author: mark.gilbert@ukaea.uk

Abstract:

Inventory calculations have a key role to play in designing future fusion power plants because they can predict the time evolution in chemical composition and hence radioactivity, including decay heat and gamma-dose, for a material exposed to neutron irradiation. For conceptual designs of the European DEMO fusion reactor such calculations provide information about the neutron shielding requirements, maintenance schedules, and waste disposal prospects; thereby guiding future development.

Extensive neutron-transport and inventory calculations have been performed for a reference DEMO reactor model with four different tritium-breeding blanket concepts. The results have been used to chart the post-operation variation in activity and decay heat from different vessel components, including a complete nuclide-by-nuclide breakdown, demonstrating the varying performance of the different blanket concepts and highlighting the problematic radionuclides.

Waste classifications, based on UK regulations have also been applied to the inventory results to predict the likely growth and decay of waste in different classes. The large mass of the vacuum vessel will not be classifiable as low level waste on the 100-year timescale, but the majority of the divertor will be, while both components will be potentially recyclable within that time.

1 Introduction

During operation of a DEMOnstration fusion power plant a large flux of 14 MeV neutrons will be generated within the burning plasma, causing structural damage and activation in the surrounding reactor vessel. The material activation, in particular, is problematic because the associated radiation fields can severely hamper maintenance operations, and the cost of disposal and recycling prospects of waste at the end of reactor lifetime is one of the primary considerations when assessing the commercial viability of fusion power.

It is therefore important to perform analyses during the conceptual designing of DEMO to ensure that the shutdown activation, decay-heat, and radioactive waste are minimised. Inventory calculations can predict the time evolution in composition, activation, decay heat, γ-dose, gas production, and even damage (dpa) dose. Combined with neutron transport calculations of DEMO designs (to define the neutron fields) such calculations can provide information about the neutron shielding requirements, possible maintenance schedules, and waste disposal prospects, thereby guiding future development.

The present paper describes calculations of post operation activation and decay heat of vessel components, as well as predictions of the build-up and radioactive waste of the entire reactor model, and if and when that waste might be recyclable. Comparison of results from a DEMO model with four different

breeder-blanket concepts allows for a basic analysis of the likely implications of a particular choice on the activation of components, including the differing shielding performance of each option.

2 Calculations

Neutron transport simulations have been performed using MCNP6.1 [1] for a conceptual model of DEMO created within the European DEMO studies programme in 2014 (developed as part of [2], but see also, for example [3, 4]). The model has homogenized tritium blanket modules, and the fixed blanket thickness allows for a direct comparison of the relative shielding characteristics of the different concepts in identical geometric configurations. A schematic of the finite-element geometry of the DEMO design used within MCNP is shown in figure 1.

Four tritium-breeding concepts have been considered in this study(see [5] for more details):

- HCLL – a helium-cooled system with a liquid lithium-lead blanket;
- HCPB – helium-cooled with a ceramic pebble-bed of Be and Li orthosilicate);
- WCLL – water-cooled with liquid lithium-lead;
- DCLL – a dual coolant reactor with a self-cooling liquid lithium-lead blanket and helium cooling elsewhere.

In all cases the divertor is water cooled with a 5 mm tungsten plasma-facing layer (also used for the 2 mm first wall armour). EUROFER is the primary in-vessel structural steel, while in other regions, including in the vacuum vessel (VV) walls, SS316L(N)-IG is used.

For each version of the model, 10^9 neutron histories were simulated in MCNP, which produced sufficient statistics for neutron spectra recorded in the finite-element cells of interest. The nuclear interactions in the simulations were governed by the FENDL-2.1 [8] neutron-reaction cross section library, with supplementary information from the ENDF/B-VII.1 [9] library for nuclides absent from FENDL-2.1. Figure 2 shows some typical spectral results obtained, in this case for a series of locations at increasing depths into the outboard equatorial wall of the HCPB concept. The first wall (FW) armour is nearest to the plasma, followed by, in increasing depth order, FW, blanket, manifold, and VV. The figure illustrates the drop in total flux as the neutrons are gradually moderated and absorbed, which also causes a softening of the spectra.

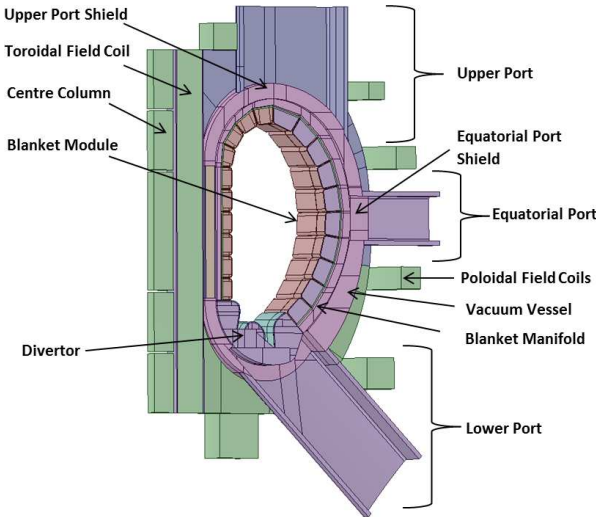

FIG. 1: A schematic of the 11.25° sector DEMO model used for the neutron transport simulations.

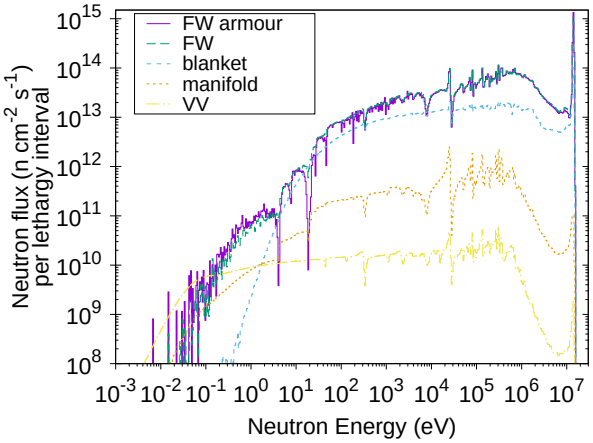

FIG. 2: Neutron energy spectra simulated for the HCPB concept in different regions of the outboard equatorial first wall, plotted as fluxes per lethargy interval.

The neutron spectra tallies have been used in a sequence of detailed inventory simulations performed with the FISPACT-II [7] system using the EAF-2010 [10] neutron-reaction cross section library and associated decay data. The material in each non-empty cell of the geometry was irradiated according to the full 2-phase operation scenario envisaged for DEMO (see [11]) under the neutron spectrum predicted for

that cell. A 1 year shutdown was assumed between phases 1 and 2 (for blanket and divertor replacement), with 8 month shutdowns for the two divertor replacements in phase 2.

The waste classification analyses performed in this work (see section 4) required further that additional inventory simulations be performed for the cells of the blanket and divertor, to match the number of times they are to be replaced – a removed component will still contribute to the overall waste inventory as it cools, but shifted in time relative to the components in the reactor at end-of-life (EOL). At the end of the operational phase a sequence of decay-cooling steps were modelled to define activities after final DEMO shutdown.

The resulting set of FISPACT-II outputs contains detailed nuclide inventory breakdowns as a function of concentration and radiological response, as well as total activities, decay-heats, γ-doses, etc., at each time-step (plasma-operation or shutdown). Where appropriate, results have been summed or averaged as a function of reactor component, for example, over all cells of the VV, with a cell's volume and density (from the MCNP model) used to define its mass scaling factor. Selected results, focusing in particular on comparisons between the four DEMO-blanket concepts, are presented below.

3 Results: Activity and decay heat

Figure 3 shows the poloidal variation in total activity and decay heat in the VV of the DEMO model with the four blanket concepts 4 weeks after the final DEMO shutdown. As expected, the highest activity is in the inboard equatorial VV. The significantly worse result for VV regions behind the tritium breeding blanket of the HCLL concept is a potential cause for concern. It suggests that the HCLL (and to a lesser extent DCLL) concept would require more shielding to protect the VV than either HCPB or WCLL. However, since the shielding and blanket design of the geometry used for these calculations was optimised for the HCPB concept, it may be that this prediction is mitigated in a properly optimised concept. The activation behind the divertor cassette is identical in all four DEMO-blanket concepts, which is expected since the divertor cells do not differ.

The relative comparison between the different cells of the VV does not change with time, so it is instead more useful to examine the time-evolution. Figure 4 shows the time-evolution after shutdown in per-kg activity and decay heat, averaged across all cells of the VV. It demonstrates that the activation of the material contained in the VV (predominantly a 80% SS316, 20% water by volume mix) falls by several orders of magnitude after only a few years. As in figure 3, the activation of the VV behind HCLL blanket modules is the highest at all decay times, with the HCPB and WCLL concepts, in particular, producing almost an order of magnitude lower per kg activities and decay heats at all times. It is interesting to note that the curves and data points for HCPB and WCLL in the figure are almost indistinguishable – in agreement with figure 3 –, which is somewhat surprising given the different material compositions of the blankets that the majority of neutrons have passed through before reaching the VV.

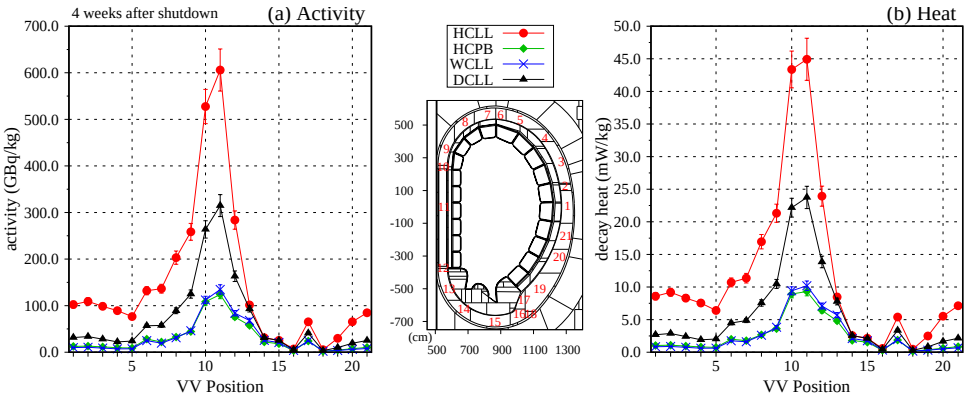

FIG. 3: Poloidal variation in (a) total activity in GBq kg^{-1}, and (b) decay heat in mW kg^{-1}, of the VV four weeks after final DEMO shutdown. Results are shown for all four DEMO-blanket concepts. The toroidal cross section through the MCNP geometry indicates the position of the numbered VV cells in the plots.

Using the full inventory output from FISPACT-II at each time-step, it is also possible to define the time-evolving nuclide contributions to the calculated total activity and decay heat. Figure 5 shows how the activity of the most important radionuclides varies with time during decay for the VV in the

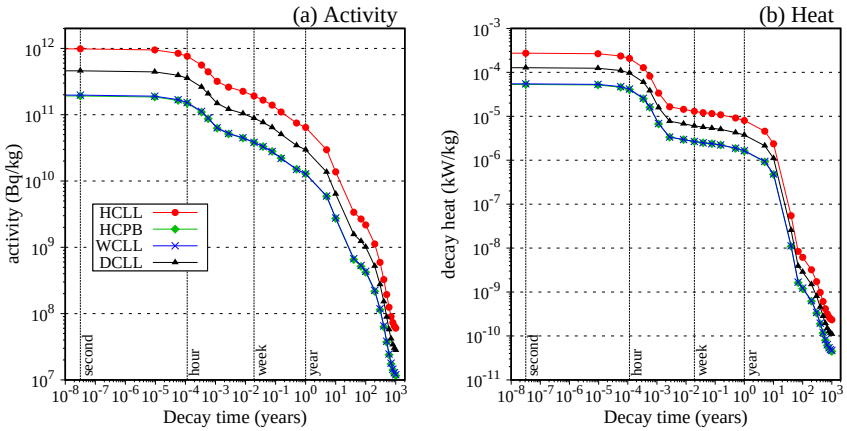

FIG. 4: Decay profile of (a) activity, and (b) decay heat, averaged (by cell mass) across all VV cells.

HCLL concept (results for the other blanket concepts are similar but on different absolute scales) – again, mass-averaged across all VV cells.

For activity (figure 5a), it can be seen that at short timescales the most dominant radionuclide is ^{56}Mn. At longer times, greater than 1 day, first ^{51}Cr and then ^{55}Fe become the most dominant nuclides, with half-lives of 27.7 days and 2.7 years, respectively. While ^{55}Fe is unavoidable, the contribution from ^{51}Cr, on the other hand, could be reduced if the concentration of Cr, responsible for the majority of its production, were lowered. Indeed, the reduced-activation EUROFER steel has significantly less Cr than SS316, and we shall see below in the divertor analysis that the ^{51}Cr contribution is largely absent (figure 7).

At very long times – greater than 10 years–, the dominant contribution from ^{63}Ni originates from the relatively high Ni content (12.5 weight %) of SS316. The decay heat radionuclide contributions in figure 5b are noticeably different to the activity results at medium timescales between 1 day and 10 years. It is ^{60}Co, instead of either ^{55}Fe or ^{51}Cr, that dominates the heat produced from the material.

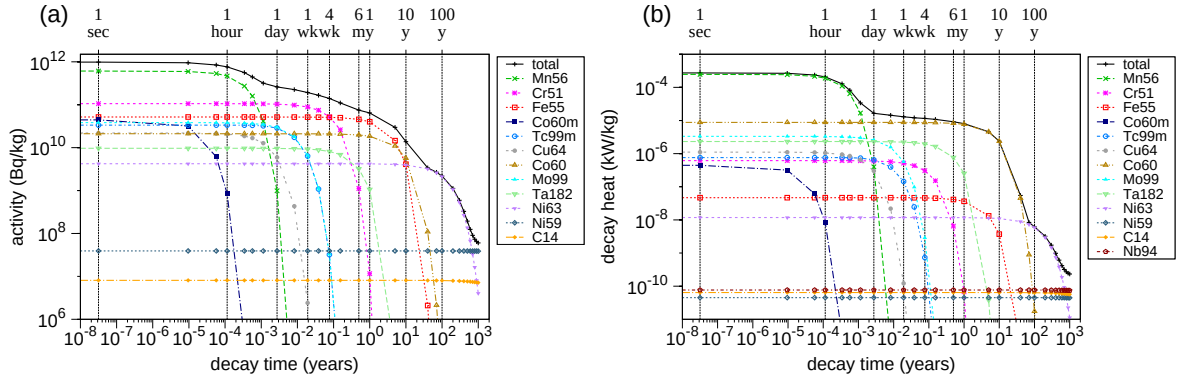

FIG. 5: Radionuclide breakdown of the decay-profile of (a) activity, and (b) decay heat, averaged (by cell mass) across all VV cells in the HCLL concept.

Figure 6 shows a typical poloidal variation for the different cells of the divertor body – in this case at 1 second after shutdown in the "phase 2c" divertor present in the DEMO vessel at EOL. As with the VV results in the previous section, there is very little change in this profile with time. The figure demonstrates that cells more exposed to neutrons (rather than waste gases), become more activated than cells that are better shielded. As expected, the activation is almost the same in each of the four blanket concepts (figure 6).

Initially, the activation in the EUROFER divertor body is higher than in the SS316 of the VV. However, at longer times the reverse is true – the EUROFER steel of the divertor body is less active than the SS316 steel, particularly at timescales on the order of 100 years and beyond. Examining the nuclide contributions for the divertor body in the HCPB concept (figure 7) reveals that the long-lived ^{63}Ni isotope, which dominated the long-term activity of the VV (figure 5), is no longer important in EUROFER. This is due to the much lower concentration of Ni in the starting composition of EUROFER

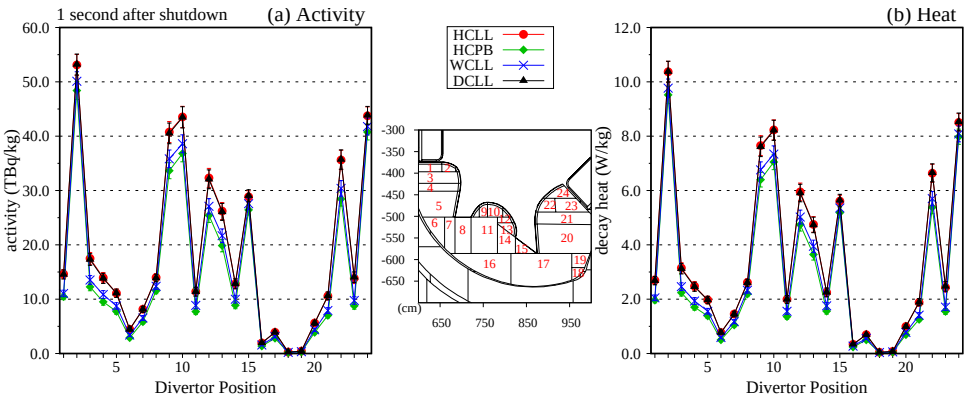

FIG. 6: Poloidal variation in (a) total activity in TBq kg^{-1}, and (b) decay heat in mW kg^{-1}, of the final replacement divertor body one second after DEMO shutdown. Results are shown for all four DEMO-blanket concepts. The toroidal cross section through the MCNP geometry indicates the position of the numbered divertor cells in the plots.

in comparison to SS316. The long-term activation in EUROFER is, instead, dominated by ^{14}C (for activity) or ^{94}Nb (decay heat).

EUROFER does not perform as well at short decay times because of the 1.2 atm.% W. Figure 7 shows that the ^{187}W produced from W under irradiation causes significant activity, and to a lesser extent decay heat, during the first day following EOL shutdown, which could have implications if immediate remote maintenance of the divertor is required.

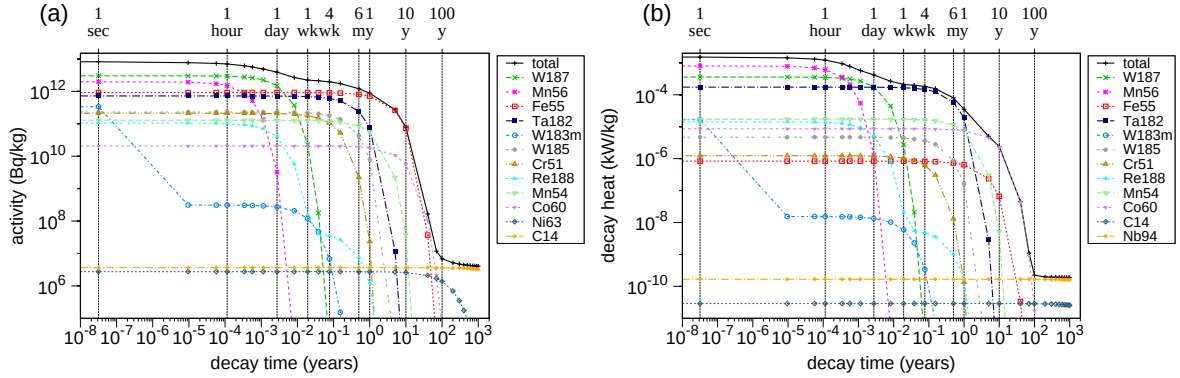

FIG. 7: Radionuclide breakdown of the decay-profile of (a) activity, and (b) decay heat, averaged (by cell mass) across all divertor body cells in the HCPB concept.

The armour of the divertor is almost entirely W, and so the problem with^{187}W is even more significant – as demonstrated by the nuclide contributions to the activation of the HCPB concept (figure 8). Beyond 10 years, radionuclides such as ^{60}Co and ^{39}Ar, produced from the minor impurities of the nominally pure W (99.7 atm.%), contribute the majority of the activity at longer times. This potentially illustrates the need to pay more attention to the fabrication of W for near plasma regions to reduce the concentration of the minor impurities that produce these radionuclides.

Figure 9 shows the poloidal variation in activity in the divertor armour at two different times after DEMO shutdown. After 1 hour (figure 9a), there is a significant difference between the four DEMO-blanket concepts, but by 1 year after shutdown (figure 9b) the differences have largely disappeared.

4 Results: Waste classification

Predicting the amount of waste produced from DEMO is vital to assess the likely environmental impact, which should be minimised, and disposal costs of DEMO, and also to secure regulatory approval. Using preliminary waste classifications (currently under review within Europe), based on UK regulations [12], for IAEA waste classes [13], it is possible to trace the time-evolution in waste masses in each class using

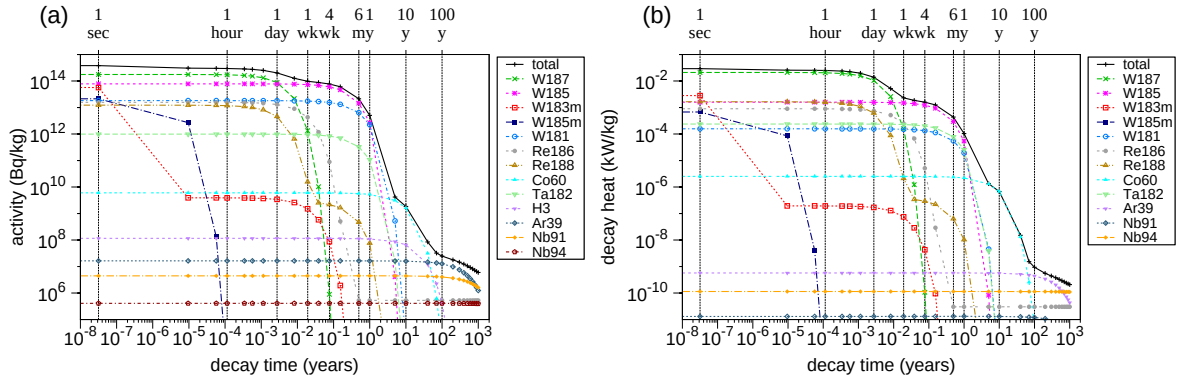

FIG. 8: Radionuclide breakdown of the decay-profile of (a) activity, and (b) decay heat, averaged (by cell mass) across all final-replacement divertor armour cells in the HCPB concept.

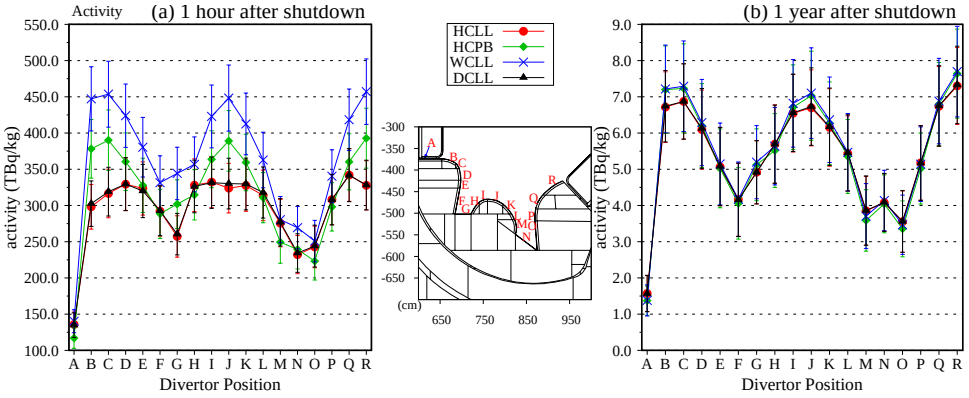

FIG. 9: Poloidal variation in total activity in TBq kg^{-1} of the divertor armour (a) one hour, and (b) one year, after final DEMO shutdown. Results are shown for all four DEMO-blanket concepts.

the inventory output, both during operation and after shutdown. The mass of material in every cell of the geometry was attributed to waste classes at each time-step using the following definitions and limits:

- NAW – none active waste. Material falls into this category if its IAEA clearance index [14] is at or below 1. Clearance index is a standard output per nuclide from FISPACT-II;
- LLW – low level waste. Categorised as material with α activity of less than 4 MBq kg^{-1} and a combined $\beta + \gamma$ activity of less than 12 MBq kg^{-1}. FISPACT-II breaks-down the activity of each nuclide according to their established decay schemes, making comparisons against these limits straightforward;
- ILW – intermediate level waste. Material with activities above the LLW limits.

It was assumed that there was no high level waste (HLW). Where a component was replaced during operation, both the removed mass and its replacement were added to the appropriate waste class as a function of time. In addition to the waste classifications there was also a preliminary assessment of the recyclability of components. A component was recyclable material (RM) if the contact γ-dose rate (calculated by FISPACT-II [7]) was below 2 mSv hr^{-1} – a level below which the material could be manipulated by remote handling equipment without their electronics being too severely damaged.

Most material of the DEMO model, including all of the VV and divertor, is predicted to be ILW during operational lifetime and for the first few decades following EOL. After shutdown, the LLW class grows until it eventually becomes the majority. The actual position of the cross-over between the ILW and LLW classes varies between the four DEMO-blanket concepts with HCPB having an earlier cross-over. In all concepts the VV remains mostly ILW for several hundred years after shutdown. For HCLL this situation is particularly bad, with virtually none of the VV classifiable as LLW, even after 1000 years. For all four concepts, very little of the waste from the modelled regions (in-vessel blanket and divertor, VV, and certain ex-vessel components) is classifiable as NAW.

Figure 10 shows the typical waste and recycling classification results for the HCPB divertor body and PFCs. Virtually all of the waste mass is ILW at shutdown and the divertor PFCs remain largely ILW even at 1000 years. Note that the divertor PFCs include both the W armour and the cooling layer, containing Cu and water, beneath it. For the divertor body, on the other hand, in figure 10b the waste is predicted to cool enough to become almost entirely LLW between around 10 and 100 years, which is exactly the timescale over which ^{55}Fe and ^{60}Co decay away (see figure 7). Despite these differences the recycling-mass estimates for the divertor PFCs and body in figures 10 show similar results. In both cases the components are predicted to become potentially recyclable within 100 years. For the VV the situation is the same, with the entire mass of SS316 steel potentially RM within 100 years.

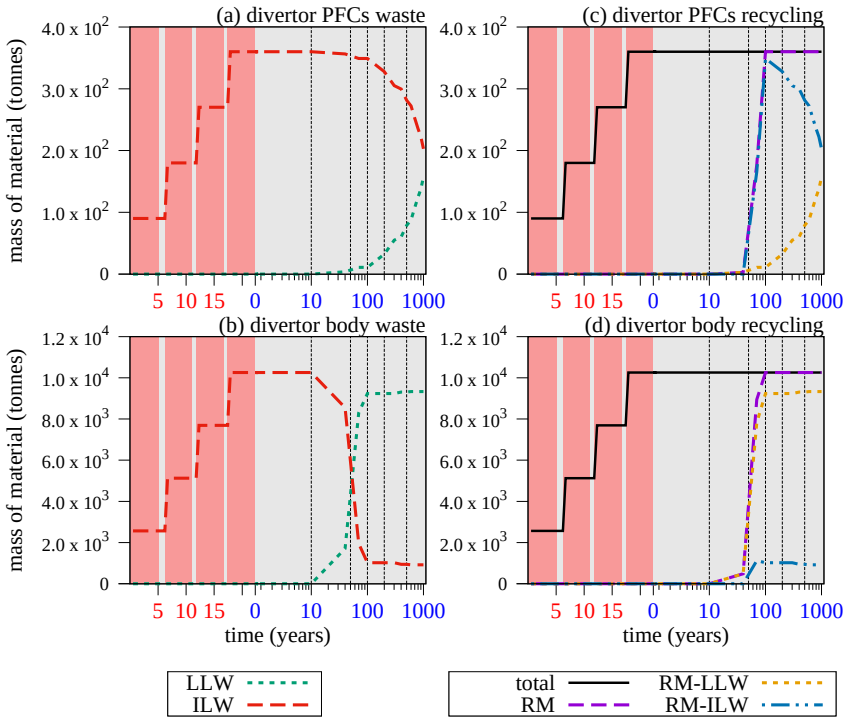

FIG. 10: Time evolution in waste (a and b) and recyclable (c and d) masses for the HCPB divertor PFCs (a and c) and divertor body (b and d). The red regions in the plots indicate periods of operation and the grey regions represent shutdown and maintenance periods. The red time axis labels refer to the operational phase on a linear scale and the blue labels the EOL shutdown on a logarithmic scale. To aid visualization, vertical gridlines are shown at 10, 50, 100, 200, and 500 years beyond EOL. Total material masses and waste separation of RM are also given in c and d.

5 Summary

Extensive neutron-transport and inventory simulations have been performed for four DEMO-blanket concepts with different tritium breeding blanket options in identical reactor geometries. The resulting predictions have been used to assess and compare the activation and decay-heat of the vacuum vessel (VV) and divertor of the European DEMO design after the expected operational lifetime. Additionally, the waste production prospects of the reactor geometry have been investigated using a preliminary classification system based on IAEA and UK guidelines.

In the fixed geometry of the DEMO model the helium-cooled lithium-lead (HCLL) blanket modules provide significantly less shielding, leading to greater activation in the VV. This suggests that, for the present DEMO design, the HCLL (and to a lesser extent dual-cooled lithium-lead, DCLL) blanket concept would require additional design-optimisation to achieve the same neutron-shield protection as provided by either the HCPB or WCLL concepts.

Component-averaged radionuclide inventories, which are similar for all four reactor concepts, for the plasma-facing armour of the divertor suggest that the minor impurities present in the manufacturing specifications of “pure” W create long-lived activation products, indicating the need for careful control of material compositions. Meanwhile, in the EUROFER steel of the divertor and the SS316 steel of the

VV, the usual short-lived radionuclides (^{55}Fe, ^{56}Mn) dominate at short decay-timescales. However, at longer times there are noticeable variations caused by subtle differences in the compositions of the steels, and SS316 performs badly, producing not only more ^{60}Co than EUROFER, but also long-lived nuclides of Ni.

Waste classification predictions, which included all components modelled in the geometry, indicate that the majority of the DEMO vessel, but particularly the steel of the VV and divertor, will remain as intermediate level waste (ILW) for many decades after shutdown before beginning to cool sufficiently to begin reclassification as low level waste (LLW). However, neither the VV or in-vessel components (blanket and divertor) cool sufficiently in 1000 years to satisfy the IAEA clearance index limit for none active waste (NAW), and the tungsten armour of the divertor remains largely ILW on this timescale. After around 100 years, the VV and divertor are predicted to be recyclable for all DEMO reactor designs. Note that the homogenization across the thickness of the VV in the present DEMO model significantly overestimates the activity of outer VV regions (far from the plasma), while underestimating inner regions. This could significantly alter the predictions made here, and so an analysis of a more heterogeneous VV is part of ongoing work.

This work has been carried out within the framework of the EUROfusion Consortium and has received funding from the Euratom research and training programme 2014-2018 under grant agreement No 633053 and from the RCUK Energy Programme [grant number EP/I501045]. To obtain further information on the data and models underlying this paper please contact PublicationsManager@ccfe.ac.uk. The views and opinions expressed herein do not necessarily reflect those of the European Commission.

References

[1] MCNP6 User Manual, Version 1.0, 2013; Edited by D. B. Pelowitz, Los Alamos document number: LA-CP-13-00634, Rev. 0. Further details at `http://mcnp.lanl.gov/`

[2] Villari R, Neutron shielding study of the DEMO upper vertical port, 2APSUF, EUROfusion, 2014

[3] Federici G, et al., 2016, *Nucl. Fus.* to be published

[4] Bachmann C, et al., 2015, *Fus. Eng. Des.*, **98–99** 1423–1426

[5] Federici G, Kemp R et al., 2014, *Fus. Eng. Des.*, **89** 882–889

[6] Davis A and Turner A, 2011, *Fus. Eng. Des.*, **86** 2698–2700

[7] Sublet J -Ch et al., The FISPACT-II User Manual, CCFE-R(11) 11 Issue 7, CCFE, 2015

[8] López Aldama D and Trkov A, FENDL-2.1: Update of an evaluated nuclear data library for fusion applications, INDC(NDS)-467, IAEA, 2012

[9] Chadwick M B et al., 2011, *Nuclear Data Sheets*, **112** 2887–2996 Special Issue on ENDF/B-VII.1 Library. See `http://t2.lanl.gov/nis/data/endf/`

[10] Sublet J -Ch et al., The European Activation File: EAF-2010 neutron-induced cross section library, CCFE-R(10)05, 2010 Available from `http://www.ccfe.ac.uk/EASY2007.aspx`

[11] Harman J, DEMO Operational Concept Description, 2LCY7A, EUROfusion/EFDA, 2012

[12] Strategy for the management of solid low level radioactive waste from the non-nuclear industry in the United Kingdom, , Department of Energy & Climate Change, UK, 2012

[13] IAEA Safety Standards: Classification of Radioactive Waste, General Safety Guide: GSG-1, IAEA, Vienna, 2009

[14] Clearance levels for Radionuclides in Solid Materials: Application of the Exemption Principles, IAEA-TECDOC-855, IAEA, Vienna, 1996